Journal of Engineering Mathematics, Vol. 6, No. 2, April 1972
Wolters-Noordhoff Publishing–Groningen
Printed in the Netherlands

Switched Numerical Shuman Filters for Shock Calculations

A. HARTEN AND G. ZWAS

Department of Mathematical Sciences, Tel Aviv University, Israel

(Received June 14, 1971 and in revised form July 20, 1971)

SUMMARY

When using Shuman's filtering operator in the numerical computation of shock waves, nonlinear instabilities are prevented, but high order accuracy is lost even in smooth regions. In order to preserve second or higher order accuracy in these regions, an automatic switched Shuman filter is constructed. Nonsteady shock calculations in one and two spatial dimensions, demonstrate the usefulness and accuracy of the method, including examples with third and fourth order accurate finite difference schemes.

1. Introduction

In [1] Vliegenthart has shown how to apply Shuman's method of filtering short wave components for shock calculations. Taking a quasi-linear hyperbolic system in conservation form, namely

$$U_t = [F(U)]_x \qquad ([F(U)]_x \equiv A(U)\cdot U_x)\,, \tag{1}$$

Vliegenthart uses the following finite difference scheme

$$U_i^{n+1} = (\tilde{U}_{i+1}^n + \tilde{U}_{i-1}^n)/2 + \frac{\lambda}{2}(\tilde{F}_{i+1}^n - \tilde{F}_{i-1}^n) \tag{2a}$$

$$U_i^{n+2} = \tilde{U}_i^n + \lambda(F_{i+1}^{n+1} - F_{i-1}^{n+1}) \tag{2b}$$

$$= (U_{i+1}^{n+2} + 2U_i^{n+2} + U_{i-1}^{n+2})/4 \tag{2c}$$

where

$\lambda = \Delta t/h$ $(h = \Delta x)$, and $U_i^n = U(ih, t_n)$.

The first two difference equations form the second order accurate two step method due to Richtmyer; (2c) is a Shuman filtering operator which reduces the accuracy everywhere to first order. $\tilde{U}_i^{n+2}$ is taken as the numerical solution at $x_i = ih$ and $t_{n+2} = t_n + 2\Delta t$.

In two spatial dimensions the system is,

$$W_t = [F(W)]_x + [G(W)]_y \tag{3}$$

where $F_x \equiv A\cdot W_x$ and $G_y \equiv B\cdot W_y$. The scheme suggested in [1] for solving (3) is:

$$W_{ij}^{n+1} = (\tilde{W}_{i+1,j}^n + \tilde{W}_{i-1,j}^n + \tilde{W}_{i,j+1}^n + \tilde{W}_{i,j-1}^n)/4 + \\ + \frac{\lambda}{2}(\tilde{F}_{i+1,j}^n - \tilde{F}_{i-1,j}^n) + \frac{\lambda}{2}(\tilde{G}_{i,j+1}^n - \tilde{G}_{i,j-1}^n) \tag{4a}$$

$$W_{ij}^{n+2} = \tilde{W}_{ij}^n + \lambda(F_{i+1,j}^{n+1} - F_{i-1,j}^{n+1}) + \lambda(G_{i,j+1}^{n+1} - G_{i,j-1}^{n+1}) \tag{4b}$$

$$\tilde{W}_{ij}^{n+2} = (W_{i+1,j}^{n+2} + W_{i-1,j}^{n+2} + W_{i,j+1}^{n+2} + W_{i,j-1}^{n+2})/4\,. \tag{4c}$$

Vliegenthart found that these schemes, although producing first order accuracy results, yield much sharper shocks than with the staggered-Lax scheme (see [7]) and other first order schemes.

We suggest here the use of the same Shuman method in a selective fashion, namely to construct schemes that will *automatically* switch-on the numerical filter *only* at the shock waves.

By doing so, the order of the basic scheme is preserved except at shock regions, even when the basic accuracy is of an order higher than the second.

In this way it will be possible to construct different schemes which are especially suitable for solving hyperbolic systems with discontinuous solutions.

All the numerical results reported herein were calculated with a CDC-6600 computer at the Tel-Aviv University computation center.

2. The One-Dimensional Case

Let L be the basic finite difference operator of second (or higher) order accuracy, and consider the scheme

$$W_i^{n+1} = L \cdot \tilde{W}_i^n \tag{5a}$$

$$\tilde{W}_i^{n+1} = W_i^{n+1} + \tfrac{1}{4}[\theta_{i+\frac{1}{2}}^{n+1}(W_{i+1}^{n+1} - W_i^{n+1}) - \theta_{i-\frac{1}{2}}^{n+1}(W_i^{n+1} - W_{i-1}^{n+1})], \tag{5b}$$

where θ is the automatic switch. If $\theta \equiv 1$ then (5b) is a simple Shuman filter. It is of importance to introduce θ in a conservation form in order to assure correct shock velocities. The right-hand side of (5b) approximates $[W + \frac{1}{4}h^2(\theta W_x)_x]_i^{n+1}$ and is therefore in conservation form.

Let us first take L to be the Lax–Wendroff scheme [2] in which case (5a) takes the form

$$W_i^{n+1} = \tilde{W}_i^n + \frac{\lambda}{2}(\tilde{F}_{i+1}^n - \tilde{F}_{i-1}^n) + \frac{\lambda^2}{2}[\tilde{A}_{i+\frac{1}{2}}^n(\tilde{F}_{i+1}^n - \tilde{F}_i^n) - \tilde{A}_{i-\frac{1}{2}}^n(\tilde{F}_i^n - \tilde{F}_{i-1}^n)] \tag{6}$$

where $A_{i+\frac{1}{2}}^n = A((\tilde{W}_{i+1}^n + \tilde{W}_i^n)/2)$.

The automatic switch θ will be of a pseudo viscosity type but so normalized that

$$\theta = \begin{cases} O(1) & \text{in shock regions}, \\ O(h^{r-1}) & \text{in smooth regions}, \end{cases} \tag{7}$$

where r is the order of accuracy of L (in (6), $r=2$). The structure of θ will be dealt with later but we already see that in smooth regions $\tilde{W}_i^{n+1} = W_i^{n+1} + O(h^{r+1})$ and the order of accuracy is preserved.

The linear stability analysis is performed in the usual way, taking the matrix A to be locally constant. Let us denote by G_k and $\tilde{G}_k$ the amplification matrices corresponding to the linearized difference operator L (taken from (5a)) and the over-all linearized operator $\tilde{L}$ ((5a) substituted into (5b) after linearizing).

Using the same approach as Von-Neumann and Richtmyer (see [3] or [4] §12.12) we treat θ as being locally constant while performing the Fourier transform and only afterwards will θ's variation be taken into account due to the fact that θ will be a nonnegative dimensionless *bounded* quantity. The bound, as we shall see later, is $2/d$ where d is the number of spatial dimensions.

If we now denote by S the amplification matrix corresponding to the filtering step (5b), we find that

$$S = \left(1 - \theta \sin^2 \frac{\xi}{2}\right) I \tag{8}$$

and

$$\tilde{G}(\tilde{L}) = S \cdot G(L) \tag{9}$$

where $\xi = k \cdot h$ is the dual variable after the usual Fourier transform and k is any Fourier frequency. As Vliegenthart [1] pointed out, S has a damping effect and since it is real the phases of the Fourier components are unaffected. If we now impose $0 \leqq \theta \leqq 2$ then for every ξ, $|\xi| \leqq \pi$,

$$\left|1 - \theta \sin^2 \frac{\xi}{2}\right| \leqq 1 \tag{10}$$

and since $\tilde{G}(\tilde{L}) = (1 - \theta \sin^2 \frac{1}{2}\xi) G(L)$ the stability of L implies the stability of $\tilde{L}$. If L is the Lax–Wendroff operator, this will mean that the criterion

$$\lambda = \frac{\Delta t}{h} \leqq \frac{1}{\rho(A)} \quad (\rho(A) = \text{largest eigenvalue of } A)\,, \tag{11}$$

assures linear stability also for the compound scheme ((5a)+(5b)) provided $0 \leqq \theta \leqq 2$.

3. The Two-Dimensional Case

When dealing with several spatial dimensions, we shall insert switched numerical filters, one for each dimension. In two dimensions we write,

$$W_{ij}^{n+1} = L \cdot \tilde{W}_{ij}^{n} \tag{12a}$$

$$\begin{aligned}\tilde{W}_{ij}^{n+1} = W_{ij}^{n+1} &+ \tfrac{1}{4}[\theta^x_{i+\frac{1}{2},j}(W_{i+1,j}^{n+1} - W_{ij}^{n+1}) - \theta^x_{i-\frac{1}{2},j}(W_{ij}^{n+1} - W_{i-1,j}^{n+1})] \\ &+ \tfrac{1}{4}[\theta^y_{i,j+\frac{1}{2}}(W_{i,j+1}^{n+1} - W_{ij}^{n+1}) - \theta^y_{i,j-\frac{1}{2}}(W_{ij}^{n+1} - W_{i,j-1}^{n+1})]\,.\end{aligned} \tag{12b}$$

L can be the two-dimensional Lax–Wendroff scheme, or the Richtmyer two-step method, or any other scheme of second or higher order of accuracy. (12b) is again written in conservation form, since its right-hand side approximates $W + \frac{1}{4}h^2(\theta^x W_x)_x + \frac{1}{4}h^2(\theta^y W_y)_y$. Again, if the θ's were 1, then (12b) would coincide with (4c), the regular Shuman filter.

The linear stability analysis for two dimensions is an extension of the one-dimensional case, which gives us two-dimensional versions of (8) and (9); only this time

$$S = \left(1 - \theta^x \sin^2\frac{\xi}{2} - \theta^y \sin^2\frac{\eta}{2}\right) I\,, \tag{13}$$

where $\xi = k \cdot h$, $\eta = l \cdot h$ are the dual variables, k and l the Fourier frequencies. Imposing,

$$\left|1 - \theta^x \sin^2\frac{\xi}{2} - \theta^y \sin^2\frac{\eta}{2}\right| \leqq 1 \quad \text{for all } |\xi|;\ |\eta| \leqq \pi \tag{14}$$

leads to the condition $0 \leqq \theta^x;\ \theta^y \leqq 1$ which assures that if L is stable then so is the two-dimensional compound scheme ((12a)+(12b)).

4. The Automatic Switch

Up to now we imposed on the θ's the following properties:
(i) sensibility to shock-like discontinuities ($\theta = O(1)$ at shocks),
(ii) representation in conservation form,
(iii) absence of effect on the accuracy in smooth regions ($\theta = O(h^{r-1})$),
(iv) preservation of the linear stability of the basic scheme.

From (i), (iii) and (iv) we see that a switch θ must attain its maximum at the shock (at the strongest shock if there are a few); this maximum must be bounded by $2/d$ where d is the number of spatial dimensions.

It is also desired that on both sides of the shock region the switch will decrease sharply to $O(h^{r-1})$, where r is the order of accuracy of the basic scheme.

Let us first consider the one-dimensional case were $A = A(W)$ and where the eigenvalues of A are real since hyperbolicity is assumed. Next we consider any function of the dependent variables which is a good sensor of shocks. We select here as such a function μ, the largest eigenvalue of A; this is done only for the sake of simplicity. One possibility for θ is to use a normalized pseudo-viscosity, like:

$$\theta_{i+\frac{1}{2}} = \chi\left(\frac{|\mu_{i+1} - \mu_i|}{\underset{l}{\text{Max}}\ |\mu_{l+1} - \mu_l|}\right)^m \tag{15}$$

where $m \geqq r-1$ (property (iii)) and χ is a positive constant not larger than $2/d$. The switch (15) can be substituted into (5b) which is in conservation form; it is a dimensionless quantity which serves as a mathematical device without having any physical or pseudo physical meaning.

At the sharpest gradient within the shock region, $|\mu_{i+1}-\mu_i|=O(1)$ and $\theta=\chi$. In smooth regions $\theta=O(h^m)\leqq O(h^{r-1})$ since then $|\mu_{i+1}-\mu_i|=O(h)$. Whenever the solution contains shocks the denominator in (15) is $O(1)$, a fact that is uneffected by mesh refinements. This is so, since for suitable basic schemes, like that of Lax and Wendroff, the number of cells in a shock is independent of h, namely, refinement of the grid implies sharper shocks.

The fact that θ is normalized is very beneficial in our analysis, but can be dangerous in the following situations:

(1) When the solution is (or still is) continuous and the order of accuracy of the basic scheme is desired everywhere.

(2) When the solution contains, in addition to shocks, strong rarefactions so that there is a possibility of getting the maximum θ at a rarefaction. This will not occur for a fine enough grid since mesh refinements do sharpen shocks but do not change rarefaction gradients.

A remedy for these situations can be to insert a check which allows the use of the filter *only* for strong enough shock-like gradients. In addition a much sharper θ can be used as for example,

$$\theta_{i+\frac{1}{2}}=\chi\cdot\exp\left\{1-\left(\frac{\operatorname{Max}_l|\mu_{l+1}-\mu_l|}{|\mu_{i+1}-\mu_i|}\right)^m\right\}. \tag{16}$$

In dealing with hydrodynamic problems we can also use a method proposed by Rosenbluth (see [4] p. 313), namely, allow $\theta\neq 0$ only where compression occurs. Doing this, expression (15) takes the form,

$$\theta_{i+\frac{1}{2}}=\begin{cases}\chi\left(\dfrac{|\mu_{i+1}-\mu_i|}{\operatorname{Max}_l|\mu_{l+1}-\mu_l|}\right)^m & (\pm)(\mu_{i+1}-\mu_i)<0\,,\ \text{compression}\\[2ex] 0 & (\pm)(\mu_{i+1}-\mu_i)\geqq 0\,,\ \text{rarefaction}\end{cases} \tag{17}$$

The quantity $(\mu_{i+1}-\mu_i)$ changes sign when crossing from rarefaction (diverging characteristics) to compression (converging characteristics); the appropriate sign depends on the choice of μ and the independent spatial variable. Similarly with (16) where in both cases the maximum is taken over compression regions only. On χ we impose, $0\leqq\chi\leqq 2/d$ so that the linear stability condition is unchanged. A larger χ within this range will yield, as can be expected, smoother results but wider shocks. The best numerical results were obtained for $\frac{1}{2}\leqq\chi\leqq 1$.

These methods deal very well with cases containing several shocks. For example, problems of shallow flows over a ridge were very successfully solved with the proposed methods*. In such cases it is best to take the minimal m required by the basic accuracy, namely $m=r-1$, in order to prevent insufficient filtering at the weaker shocks.

The extension to more dimensions is done by constructing one θ for each direction. In two dimensions we define θ^x and θ^y as

$$\theta^x_{i+\frac{1}{2},j}=\chi\left(\frac{|\mu_{i+1,j}-\mu_{ij}|}{\operatorname{Max}_{l,k}|\mu_{l+1,k}-\mu_{l,k}|}\right)^m \tag{18a}$$

$$(m\geqq r-1)$$

$$\theta^y_{i,j+\frac{1}{2}}=\chi\left(\frac{|\mu_{i,j+1}-\mu_{ij}|}{\operatorname{Max}_{l,k}|\mu_{l,k+1}-\mu_{l,k}|}\right)^m \tag{18b}$$

Here $\theta\leqq\chi\leqq 1$ so that $0\leqq\theta^x;\ \theta^y\leqq 1$. The extension to three dimensions is obvious.

5. Numerical Results in One Dimension

Among the one-dimensional problems that were actually solved we will mention two sets of

* These results were obtained by U. Asher of Tel-Aviv University, who used (17) with $m=1$, with the Lax–Wendroff scheme.

examples. (1) A mathematical model-equation with a known solution used for checking our methods and the accuracy achieved in smooth regions. (2) A one-dimensional hydrodynamic shock for checking a simple engineering problem and testing the correctness of the numerical shock-speed.

First we took the equation

$$u_t + uu_x = 0 \tag{19}$$

with the initial conditions

$$u(0, x) = \begin{cases} 1 \quad , & x \leqq 0 \\ 1-x \, , & 0 \leqq x \leqq 1 \\ x-1 \, , & 1 \leqq x \leqq 2 \\ 1 \quad , & 2 \leqq x \end{cases} . \tag{20}$$

In this case there is a compression region which will yield a shock at the time $t=1$, and a rarefaction region with gradients decreasing in time. The exact solution is,

$$u(x, t) = \begin{cases} 1 & x \leqq t \\ \dfrac{1-x}{1-t} & t \leqq x \leqq 1 \\ \dfrac{x-1}{t+1} & 1 \leqq x \leqq 2+t \\ 1 & 2+t \leqq x \end{cases} \qquad (0 \leqq t < 1 \text{ continuous}) , \tag{21}$$

$$u(x\ t) = \begin{cases} 1 & x < 2+t-\tau \\ \dfrac{x-1}{t+1} & 2+t-\tau \leqq x \leqq 2+t \\ 1 & 2+t \leqq x \end{cases} \qquad (1 \leqq t \, , \ \tau = (2+2t)^{\frac{1}{2}} \text{ discontinuous}) .$$

This example was suggested to us by M. Goldberg [9]. The results after 300 time steps are

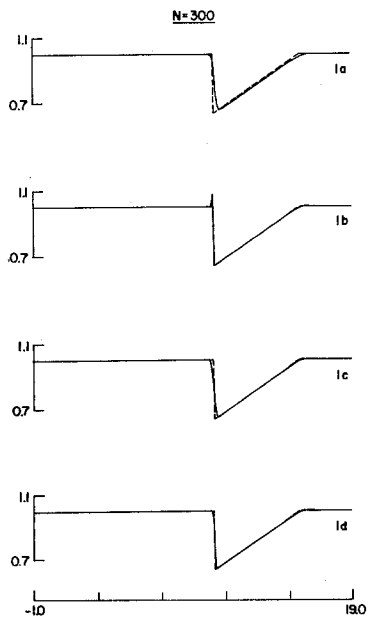

Figure 1.

plotted in Fig. 1 together with the exact solution. In all the cases we took $h=0.05$ and $0 \leqq x \leqq 20$. Graphs (1a), produced with the first order Lax scheme [7], and graph (1b) with the L–W scheme [2], are plotted for comparison purposes. It should be noted that although u is sectionally linear in x, the Lax–Wendroff term does contribute in the rarefaction region since u_{tt} does not vanish there. Graphs (1d) and (1c) show the results produced by our method with $r=2$, $m=1$, and $\chi=0.5$; 1. Notice the correctness of the shock speed and the high accuracy everywhere except at the shock itself. This high accuracy is such that the numerical values corresponding to graphs (1b) and (1d) are the same up to 6 significant decimal places in the smooth regions. By comparing (1d) with (1a) it is clear how superior our results are compared to those obtained with the first order Lax scheme, including the shock region.

The results shown in Fig. 1 were typical. Using as initial conditions for (19), a shock-like step function, again gave the correct numerical shock speed, the damping of the post shock oscillations and nearly second order shock profiles. As an example of using our method together with difference operators of orders higher than the second, we solved (19)–(20) with third and fourth order methods as basic schemes. These basic schemes are extensions of the Lax–Wendroff method constructed by Zwas and Abarbanel [8]. The Burstein–Mirin three step method [10], could also be used as the basic scheme.

In figures (2a), (2b) and (2c) we bring the results of third order accuracy with $x=0$; 0.5; 1, respectively; Figures (2d) with $x=0$ and (2e) with $x=1$ show the results obtained with a fourth order accurate scheme [8], after 300 time steps. We have used (17) with $m=3$ and the results again differ from those without filtering only in the shock region. The sharp shock and the very small errors, especially near the end of the rarefaction wave, demonstrate the high order accuracy of the basic schemes.

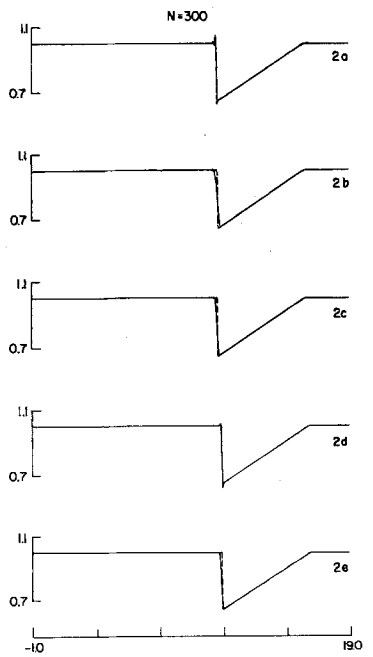

Figure 2.

6. One-Dimensional Hydrodynamics

As a second one-dimensional example the hydrodynamic system of equations in Lagrangean formulation was solved. We took the simple engineering problem of a stationary shock, moving in a polytropic gas; the equation therefore are ([4] chap. 12):

$$\begin{bmatrix} V \\ u \\ E \end{bmatrix}_t + \begin{bmatrix} -u \\ P \\ Pu \end{bmatrix}_x = 0 \quad (V_0 = 1), \tag{22}$$

Here V, u, E and P are the specific volume, the velocity, the total energy per unit mass and the pressure, correspondingly. The pressure is given by,

$$P = (\gamma - 1)(E - u^2/2)/V \tag{23}$$

where γ is the polytropic constant.

The eigenvalues of $A = \text{grad } F$, $(F^T = (u, -P, -Pu))$, are 0, $\pm c$ where c is the Lagrangean sound speed given by $(\gamma P/V)^{\frac{1}{2}}$. We used the Lax–Wendroff scheme with the switch

$$\theta_{i+\frac{1}{2}} = \begin{cases} \chi \dfrac{|c_{i+1} - c_i|}{\text{Max } |c_{k+1} - c_k|} & \text{when} \quad c_{i+1} - c_i < 0 \\ 0 & \text{elsewhere}. \end{cases} \tag{24}$$

The actual cases solved were a larger number of cases with different values of γ and different pressure ratios at the shock (namely different shock strengths) corresponding to the cases solved by Abarbanel and Zwas in [5] with other methods. Typical results are shown in Fig. 3, with $\gamma = 1.4$, pressure ratio of 10 and after 200 time steps (graph 3c). For comparison the results without filtering (3b), and with the first order Lax scheme (3a) are plotted. The shock speed for (3c) is as good as for (3b).

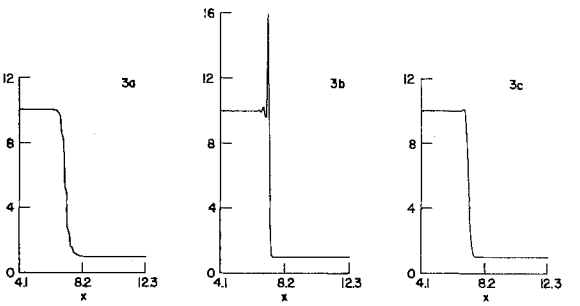

Figure 3.

The shock width with the filter (24) is almost the same for different shock strengths and polytropic constants, where as the overshoot without filtering is very much larger for strong shocks (compare with the results in [5]).

All the conclusions arrived at for the single equation (19) were found to be valid for the system (22).

Of course the Lax–Wendroff method could be used with artificial viscosity terms too ([2], [4]), but this is much more time consuming, complicated and much harder to generalize to several dimensions. This will be demonstrated in the two dimensional cases.

7. Two-Dimensional Results

We chose the example of calculating a detached shock in front of a rectangular body moving with constant supersonic speed along its axis of symmetry. This problem was suggested and solved by Burstein [6], who used the Lax–Wendroff two-dimensional scheme with two one-dimensional artificial viscosity terms. First order accurate results were obtained by Vliegenthart who used a two step method with Shuman filtering everywhere. Vliegenthart [1] found much better results than with other first order methods.

In order to submit our scheme to a real hard test we chose impulsive initial conditions, i.e., the rectangular body appeared impulsively at $t=0$ in the supersonic flow.

As our basic scheme we took the L–W method in two dimensions, as Burstein did [6], namely,

$$\begin{aligned} W_{ij}^{n+1} = W_{ij}^n &+ \frac{\lambda}{2}[(F_{i+1,j}^n - F_{i-1,j}^n) + (G_{i,j+1}^n - G_{i,j-1}^n)] \\ &+ \frac{\lambda^2}{2}\{A_{i+\frac{1}{2},j}^n[(F_{i+1,j}^n - F_{ij}^n) + \tfrac{1}{4}(G_{i+1,j+1}^n + G_{i,j+1}^n - G_{i+1,j-1}^n - G_{i,j-1}^n)] \\ &- A_{i-\frac{1}{2},j}^n[(F_{ij}^n - F_{i-1,j}^n) + \tfrac{1}{4}(G_{i,j+1}^n + G_{i-1,j+1}^n - G_{i,j-1}^n - G_{i-1,j-1}^n)]\} \\ &+ \frac{\lambda^2}{2}\{B_{i,j+\frac{1}{2}}^n[(G_{i,j+1}^n - G_{ij}^n) + \tfrac{1}{4}(F_{i+1,j+1}^n + F_{i+1,j}^n - F_{i-1,j+1}^n - F_{i-1,j}^n)] \\ &- B_{i,j-\frac{1}{2}}^n[(G_{ij}^n - G_{i,j-1}^n) + \tfrac{1}{4}(F_{i+1,j}^n + F_{i+1,j-1}^n - F_{i-1,j}^n - F_{i-1,j-1}^n)]\}. \end{aligned} \tag{25}$$

For the two-dimensional compressible polytropic fluid flow in Eulerian coordinate, W, A, B, F and G are given by:

$$W = \begin{bmatrix} \rho \\ m \\ n \\ E \end{bmatrix}; \quad A = \text{grad } F \; ; \quad B = \text{grad } G \, ,$$

$$F = -\begin{bmatrix} m \\ \dfrac{-\gamma+3}{2}\dfrac{m^2}{\rho} - (1-\gamma)\;E - \dfrac{n^2}{2\rho} \\ \dfrac{mn}{\rho} \\ \dfrac{1-\gamma}{2}\dfrac{m}{\rho^2}(m^2+n^2) + \dfrac{\gamma m E}{\rho} \end{bmatrix}; \quad G = -\begin{bmatrix} n \\ \dfrac{mn}{\rho} \\ \dfrac{-\gamma+3}{2}\dfrac{n^2}{\rho} - (1-\gamma)\;E - \dfrac{m^2}{2\rho} \\ \dfrac{1-\gamma}{2}\dfrac{n}{\rho^2}(m^2+n^2) + \dfrac{\gamma n E}{\rho} \end{bmatrix} \tag{26}$$

Here ρ, m, n and E are the density, the momentum in the x-direction (i.e., $m=\rho u$), the momentum in the y-direction (i.e., $n=\rho v$), and the total energy per unit volume; γ is the polytropic constant. The eigenvalues of A are $u, u\pm c$, and the eigenvalues of B are $v, v\pm c$, where c is here the Eulerian speed of sound given by $(\gamma P/\rho)^{\frac{1}{2}}$ and P is the pressure given by $P=(\gamma-1)[E-(m^2+n^2)/(2\rho)]$. As pointed out earlier, it is not necessary to use the eigenvalues for constructing the switches; any function which is a good sensor of shocks is suitable. We chose the following simple switches:

$$\theta_{i+\frac{1}{2},j}^x = \chi \cdot \left(\frac{|\rho_{i+1,j} - \rho_{i,j}|}{\max |\rho_{l+1,k} - \rho_{l,k}|}\right)^2 \tag{27a}$$

$$\theta_{i,j+\frac{1}{2}}^y = \chi \cdot \left(\frac{|\rho_{i,j+1} - \rho_{i,j}|}{\max |\rho_{l,k+1} - \rho_{l,k}|}\right)^2 \tag{27b}$$

where the maximum is taken over compression regions only, and χ will be specified in (29). In (27) the pressure P can replace the density if desired. The quadratic θ's were chosen to ensure sharp switches which will produce sharp shocks. The boundaries were treated according to the suggestions in [1], except that we took higher order extrapolations whose directions fall into the appropriate domain of influence.

We show below some results of stationary density profiles along lines parallel to the axis of symmetry, for different values of y. The initial conditions for the figures below were

$\gamma = 1.4$, $P = 1$, $\rho = 1$, $n = 0$, $m = 5$ (namely a Mach number of ~ 4.23), and an impulsive appearance of the body at $t = 0$. (28)

Graph (4a) shows the results with our method, graph (4b) – with Burstein's method. In both runs the geometry and mesh size were taken exactly as specified in [6].

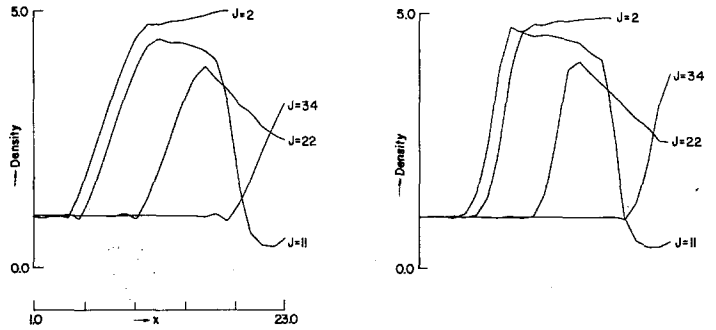

Figures 4a and b.

For the results shown in (4b) the artificial viscosity constant was taken as 2 ($\chi = 2$ in formula (5.3a) in [6]); with the value of 1, nonlinear instabilities arise and terminate the run, even when changing the constant from 2 to 1 after several hundred of cycles. The results in (4a) were obtained with (27a) and (27b) where,

$$\chi = \tfrac{1}{2} \cdot \begin{cases} 1 & \rho_{i+1,j} - \rho_{ij} > 0 \\ \alpha & \rho_{i+1,j} - \rho_{ij} \leqq 0 \end{cases} \quad \text{in (27a)} \tag{29a}$$

and

$$\chi = \tfrac{1}{2} \cdot \begin{cases} 1 & \rho_{i,j+1} - \rho_{ij} < 0 \\ \alpha & \rho_{i,j+1} - \rho_{ij} \geqq 0 \end{cases} \quad \text{in (27b)}. \tag{29b}$$

We propose to take $\alpha = 0$ in general, but for the present problem it was necessary to take a small positive α because of the strong rarefaction gradients near the corner; we have taken $\alpha = 0.1$.

The constant α should be small enough so that the θ near the corner will be much smaller than the maximal θ obtained at the shock. At all the other smooth regions, (27) yields $\theta = \theta(h^2)$, which is even one order higher than needed to ensure second order accuracy.

It is to be expected, that $\alpha = 0$ can be taken for aerodynamical bodies having continuously differentiable surfaces. The need for a small positive α in our problem is necessitated by the corner singularity.

Fig. 5 shows our results of the flow field with the stationary detached shock and sonic line, after 2000 cycles and for the initial conditions (28). Our steady state results and those of Burstein are practically identical except for small differences near the corner. These differences (Fig. 5) are much smaller for $\alpha = 0.05$. Our results show that the sonic line meets the body at the corner

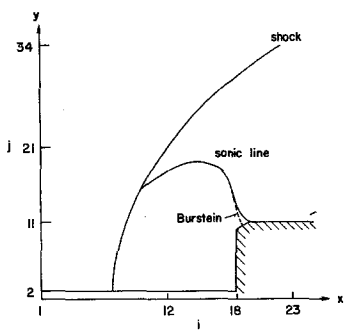

Figure 5.

in contrast to first order results where the sonic line reaches the body 3–4 cells behind the corner (see Fig. 6 in [6]).

Our results show smoother shock transitions than in [6], however the shock occupies 4–5 cells, compared to 3–4 cells when using Burstein's method (see figures (4a), (4b)). Our stagnation values were found to be closer to the exact values than those we obtained with Burstein's scheme.

Again, as with the artificial viscosity, the size of the constant χ should be chosen, so as to achieve a compromise between the smoothness and the sharpness of the profiles. For the initial conditions (28), both methods need approximately 2000 cycles in order to reach the steady state.

A great advantage of our method is in the saving of computing time; it takes less than half the time per cycle, compared to Burstein's scheme. The switched Shuman filter can be very easily extended to three dimensions, where the computing-time savings are even greater.

Two dimensional switched numerical filters can be associated with third and fourth order schemes too [11]. The accurate results in the one-dimensional case (Fig. 2) give reason to believe that this approach is promising also for several dimensions. A final remark is that switched Shuman filters can be easily added to existing computer programs in order to deal with problems containing discontinuities.

REFERENCES

[1] A. C. Vliegenthart, The Shuman filtering operator and the numerical computation of shock waves, *J. of Eng. Math.*, 4 (1970) 341–348.

[2] P. D. Lax and B. Wendroff, Systems of conservation laws, *Comm. Pure Appl. Math.*, 13 (1960) 217–237.

[3] J. Von-Neumann and R. D. Richtmyer, A method for the numerical calculation of hydrodynamic shocks, *J. of Appl. Phys.*, 21 (1950) 232–237.

[4] R. D. Richtmyer and K. W. Morton, *Difference methods for initial value problems.* Second edition, Interscience, New York (1967).

[5] S. Abarbanel and G. Zwas, An iterative finite-difference method for hyperbolic systems, *Math. Comp.*, 23 (1969) 549–565.

[6] S. Z. Burstein, Finite-difference calculations for hydrodynamic flows containing discontinuities, *J. Comp. Phys.*, 2 (1967) 198–222.

[7] P. D. Lax, Weak solutions of non-linear hyperbolic equations and their numerical computation, *Comm. Pure Appl. Math.*, 7 (1954) 159–193.

[8] G. Zwas and S. Abarbanel, Third and fourth order accurate schemes for hyperbolic equations of conservation law form, *Math. Comp.*, 25 (1971) 229–239.

[9] M. Goldberg, Ph.D. thesis, Mathematical Sciences, Tel-Aviv University.

[10] S. Z. Burstein and A. A. Mirin, Third order difference methods for hyperbolic equations, *J. Comp. Phys.*, 5 (1970) 547–565.

[11] G. Zwas and S. Abarbanel, *Third and fourth order accuracy schemes for two-dimensional hyperbolic equations,* To appear.